

## Article

# Combined Depth Control Strategy for Low-Speed and Long-Range Autonomous Underwater Vehicles

Anyuan Bi <sup>1,\*</sup>, Fengye Zhao <sup>1</sup>, Xiantao Zhang <sup>2,3</sup> and Tong Ge <sup>1,3</sup>

<sup>1</sup> School of Naval Architecture, Ocean & Civil Engineering, Shanghai Jiao Tong University, Shanghai 200240, China; zfy108@sjtu.edu.cn (F.Z.); tongge@sjtu.edu.cn (T.G.)

<sup>2</sup> State Key Laboratory of Ocean Engineering, Shanghai Jiao Tong University, Shanghai 200240, China; zhxt@sjtu.edu.cn

<sup>3</sup> Collaborative Innovation Centre for Advanced Ship and Deep-Sea Exploration, Shanghai Jiao Tong University, Shanghai 200240, China

\* Correspondence: bayst@sjtu.edu.cn

Received: 22 February 2020; Accepted: 4 March 2020; Published: 7 March 2020

**Abstract:** Autonomous underwater vehicles (AUVs) are increasingly being applied to highly detailed survey and inspection tasks over large ocean regions. These vehicles are required to have underwater hovering and low-speed cruising capabilities, and energy-saving property to enable long-range missions. To this end, a combined depth control strategy is proposed in which an on-off type variable ballast system (VBS) is adopted for satisfactory hovering or fast descending/ascending without propulsion to reach the designated cruising depth, whereas the bow and stern fins act as the actuator to maintain the cruising depth for more energy saving. A hierarchical architecture-based VBS controller, which comprises a ballast water mass planner and an on-off mass flowrate controller, is developed to assure good hovering performance of the on-off type VBS. Both numerical studies and basin tests are conducted on a middle-sized AUV to verify the feasibility and validity of this depth control strategy.

**Keywords:** autonomous underwater vehicles; depth control; variable ballast system; hierarchical architecture; on-off type mass flowrate

## 1. Introduction

With the increasingly wide activities in deep-sea exploration and exploitation, underwater vehicles of various types have become indispensable tools for scientists, researchers and engineers to conduct ocean research and perform underwater tasks [1–12]. Among them, autonomous underwater vehicles (AUVs), which are developed to provide high automation, cost-effectiveness, and medium and long-range capability to execute underwater missions without placing human lives at risk [13], are increasingly being used in highly detailed survey and inspection applications including the exploration of unknown environments [14], oceanographic observations [15], the inspection of underwater structures [16] and so on. In such scenarios, AUVs are expected to be capable of both satisfactory hovering and low-speed and energy-efficient cruising for high-quality data gathering and long-duration missions.

For most cruising AUVs, only fins are mounted and actuated with a satisfactory forward velocity to reach or keep a desired depth [17]. However, this fails for hovering or low operating speed conditions where fins will not work or cannot generate sufficient lift. The Seahorse AUV is unable to dive below the surface using the fins alone even when it is configured close to neutral buoyancy and sufficient forward speed for fin authority is achieved, due to the surface capture phenomenon and the lift forces on the nose [18]. AUVs equipped with hovering systems offer the solution [18–20].

The hovering drivers commonly adopted in underwater vehicles are vertical thrusters [15,19,21] which, although responsive, have inherent disadvantages of high energy consumption and strong perturbations to the surroundings. Alternatively, different types of variable buoyancy [20,22–24] or ballast [18,25,26] systems, which are characterized by high power efficiency and less disturbance to the environment, have been developed over the past few years. Inspired by marine animals [27], variable buoyancy systems adjust the displacement of underwater vehicles via thermal, mechanical or hydraulic mechanisms which change the temperature of enclosed oil by an electric heater [22], the volume inside a cylinder by moving a piston [20,24], and the volume of pressure-balanced oil bladder by pumping oil between a tank and a bladder [23], respectively. Variable ballast systems (VBSs), which change the masses of underwater vehicles, mainly fall into three types, i.e., water hydraulics that pump seawater between ballast tanks and the surroundings [18], compressed air that is blown/vented to/from ballast tanks [25], and the hybrid method, using both water hydraulics and compressed air [26]. With its advantages of ease in construction, sealing and disposal of working media and environmental friendliness, the water hydraulic VBS is the most popular and competitive mechanism for hovering control of AUVs [13,28].

Water hydraulic VBSs, or VBSs for short hereafter, are generally divided into two types according to whether or not the flowrate is continuously regulatable. The most widely designed type are on-off type VBSs, which can only accept three kinds of flowrate command (+1: inject water into ballast tank, −1: discharge water out from ballast tank, 0: turn off valves and close pump) without controlling the flowrate of the in/out ballast water [18,29,30]. The on-off type VBS in [18] uses a single speed motor and a fixed displacement pump, resulting in a constant pump rate, and electric valves controlling whether water is pumped into or out of each tank or whether the tanks are closed to the outside or open to seawater. The depth controller has the general form of proportional-derivative (PD) control and the depth acceleration error is quantized to generate discrete flowrate commands [18]. Although both simulations and water trials have demonstrated the effectiveness of this on-off type VBS and controller design, the hovering performance needs to be improved. Three kinds of novel VBSs—continuous type VBSs, which support the valve controlled mode via pulse width modulation (PWM) controlled solenoid valves or pump controlled mode via a servo motor to control the flowrate of ballast water—are proposed to improve the performance of an AUV hovering system [13]. Both the valve-controlled mode and pump-controlled mode, however, impose more complicated problems, to establish the mathematical models of the flowrate control means, compared to on-off type VBS. It is noteworthy that in order to realize the valve-controlled mode for continuous flowrate control [13], the electric valves (usually with a 3 s response time) used in the on-off type VBS [18] are replaced by four fast-response direct-acting solenoid valves (within milliseconds of response time), which greatly shortens the response delay of the VBS.

For hovering control at deep submergence, where underwater vehicles can be considered to be in a wave-free environment, the main challenge of controller design is to counteract the effects of modeling errors. Several different hovering control schemes have been reported. Sliding mode control (SMC) was applied for the input-output linearized submarine hovering system via compressed air VBS [25]. Model predictive control (MPC) was used to provide hover capability for a thruster-driven autonomous underwater vehicle whose model parameters were obtained experimentally [31]. However, either the exact bounds of parametric uncertainty for SMC [32] or an accurate model for MPC [33] are required. A fuzzy proportional-integral-derivative algorithm combined with a compensated dynamics equation, which needs hydrodynamics analysis and field experiments, was proposed in [34] to realize the depth control of a remotely operated vehicle in a nuclear power plant. In addition, due to its independence from the plant model and easy implementation, proportional-derivative (PD) control has been widely used in various hovering control systems [18,20,26,35], and the stability of the nonlinear system is proven using a Lyapunov-based analysis [35].

Based on the above studies, this work is devoted to the depth control system design for AUVs which are required to have capabilities of both satisfactory hovering, and low-speed and long-range cruising. To achieve this goal, a combined control strategy, which adopts bow and stern fins along

with an on-off type VBS, is presented in this paper. The VBS is used for satisfactory hovering or fast descending/ascending without propulsion to reach the designated cruising depth, whereas the more energy-efficient fins act as the actuator to counteract the remaining small vertical unbalanced force due to the on-off type VBS and maintain the cruising depth. As in [18], the on-off type VBS uses a single speed motor and a fixed displacement pump to generate a constant pump rate, while the electric valves are replaced by four fast-response direct-acting solenoid ones to improve the response performance of water flow direction control. A novel hierarchical architecture-based controller, which consists of a PD-type ballast mass planner and a flowrate controller, is proposed for the on-off type VBS to enhance the hovering performance. As for the fin control, the model-free PD controller which ensures the global asymptotic stability is applied.

The rest of this paper is organized as follows. The depth control problem of an AUV via VBS and fins is formulated in Section II. The combined depth control strategy is depicted in detail in Section III. The hierarchical on-off type VBS and the fin controllers design are presented in Section IV. Verifications of the proposed approach, including simulations and basin tests, are conducted in Section V. Finally, the paper is concluded in Section VI.

## 2. Problem Formulation of Depth Control via VBS and Fins

A typical configuration of an AUV equipped with VBS, and bow and stern fins is given in Figure 1. The schematic diagram of the on-off type VBS, which uses a single speed motor, a fixed displacement pump and four fast-response direct-acting solenoid valves, is shown in Figure 2 [13].

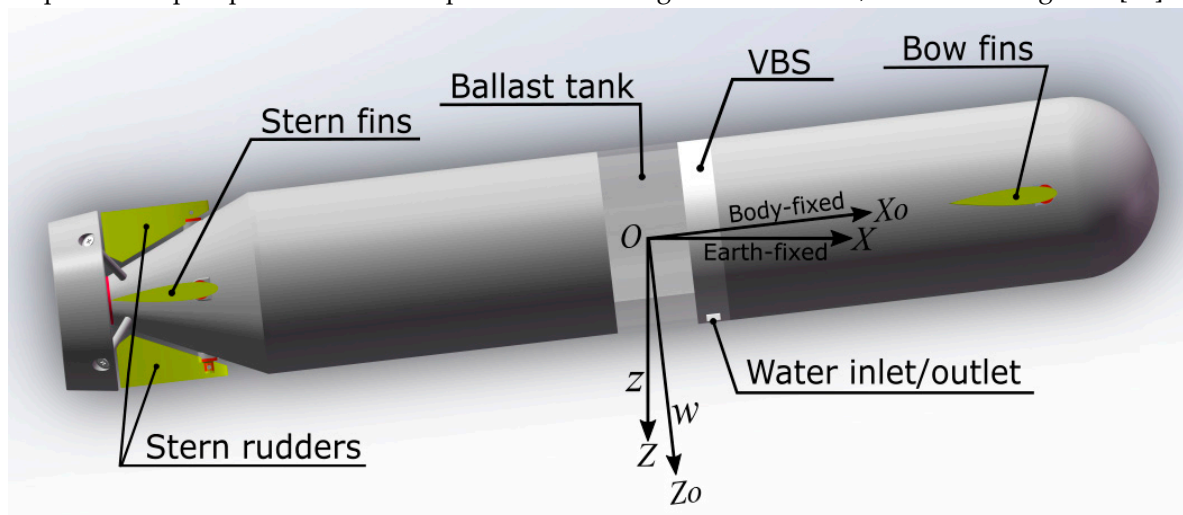


**Figure 1.** A typical configuration of an autonomous underwater vehicle (AUV) equipped with a variable ballast system (VBS) and bow and stern fins.

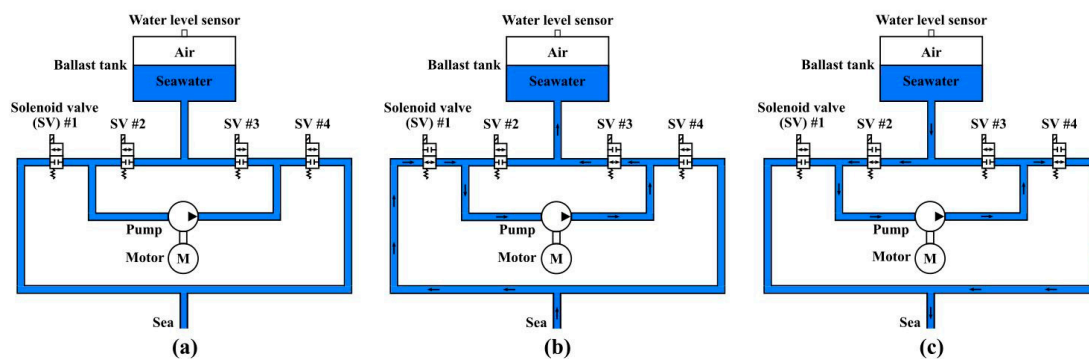


**Figure 2.** The schematic diagram of the on-off type VBS. (a) 0: close valves and turn off pump; (b) +1: open valves 1 and 3, and close valves 2 and 4; (c) -1: open valves 2 and 4, and close valves 1 and 3.

Suppose the AUV is designed to have passive stability in both roll and pitch directions, and the ballast tank is configured to have the center at the origin of the body-fixed coordinate system. When operating at a depth below the wave-affected zone, underwater vehicles are commonly modeled with constant hydrodynamic coefficients [36] and without sea wave disturbances [37]. Under these assumptions, the heave dynamics of the AUV can then be simplified as [36]

$$\begin{aligned}\dot{z} &= w, \\ (m_0 + m_a - Z_{\dot{w}})\dot{w} &= (Z_w + Z_{w|w|}|w|)w + m_a g + Z_{\delta_b}\delta_b + Z_{\delta_s}\delta_s + Z_0, \\ \dot{m}_a &= q, m_a \in [0, \bar{m}_a] \text{ \& } q \in \{-\bar{q}, 0, \bar{q}\}\end{aligned}\quad (1)$$

where  $z$  is the depth of the AUV,  $w$  is the heave velocity,  $m_0$  is the vehicle mass with empty ballast tank(s),  $m_a$  is the actual ballast mass,  $Z_{\dot{w}}$ ,  $Z_w$  and  $Z_{w|w|}$  are the constant hydrodynamic mass and the linear and quadratic damping coefficients, respectively,  $g$  is the gravitational acceleration,  $Z_{\delta_b}$  and  $Z_{\delta_s}$  are the lift coefficients of the bow and stern fins, respectively,  $\delta_b$  and  $\delta_s$  are the corresponding deflection angles of the bow and stern fins, respectively,  $Z_0$  is the vertical imbalanced force,  $q$  is the on-off type mass flowrate,  $\bar{m}_a$  is the overall mass of water contained in fully-filled ballast tank(s), and  $\bar{q}$  is the constant flowrate of the on-off type VBS.

$Z_0$  is caused by the unbalanced gravity (when the ballast tank(s) is/are empty) and buoyancy of the vehicle, and assumed to be known in prior. Note that the vehicle should be designed satisfying  $Z_0 < 0$  to enable free ascending without ballast, and  $\bar{m}_a g + Z_0 > 0$  to enable diving under the surface.

Denote the desired depth as  $z_d$ , and define the depth tracking error as  $e_z = z_d - z$ . Then, system (1) can be expressed as

$$\begin{aligned}\dot{e}_z &= -w, \\ (m_0 + m_a - Z_{\dot{w}})\dot{w} &= (Z_w + Z_{w|w|}|w|)w + m_a g + Z_{\delta_b}\delta_b + Z_{\delta_s}\delta_s + Z_0, \\ \dot{m}_a &= q, m_a \in [0, \bar{m}_a] \text{ \& } q \in \{-\bar{q}, 0, \bar{q}\}\end{aligned}\quad (2)$$

For practical hovering or cruising, the VBS or the fin controllers to be designed work accordingly, such that  $\lim_{t \rightarrow \infty} |e_z| \leq \bar{e}_z$ , where  $\bar{e}_z > 0$  is the required control accuracy.

### 3. Combined Depth Control Strategy

The combined depth control strategy is depicted in detail in Figure 3. The states of an AUV in the depth control process are denoted by circles, and each directed line/arc connecting two states represents a state transition via VBS or fins. The color of a line/arc is used to differentiate different control actions: (1) black—close-loop control via VBS without propulsion; (2) blue—close-loop control via fins with propulsion; (3) red—open-loop control via VBS without propulsion. When there is more than one way for the transition of two states, the way with the minimum number of control steps (each line/arc is a control step) is adopted.

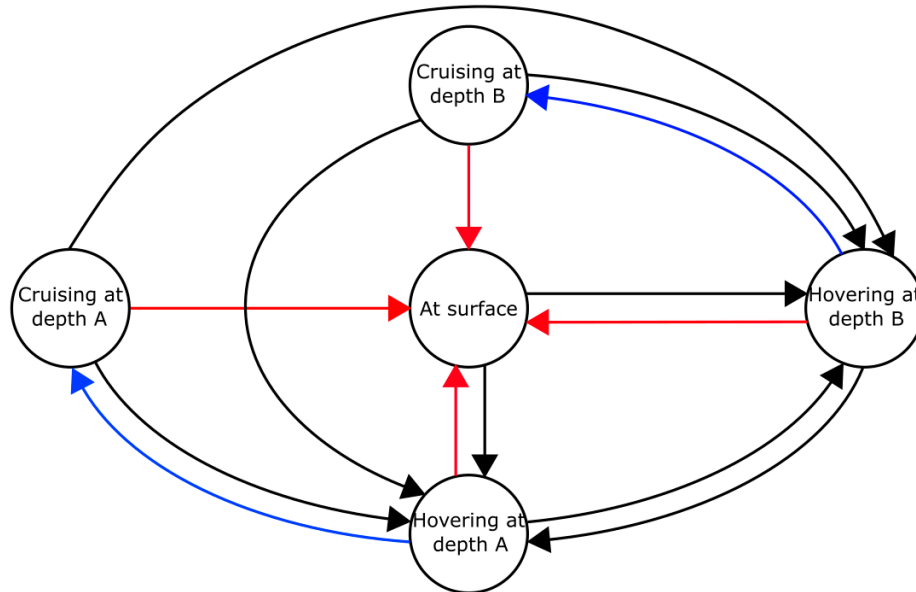


**Figure 3.** The states and transitions in the depth control process of an AUV.

It should be noted that in practical applications, hovering via VBS is achieved once the vehicle reaches a quasi-static vertical equilibrium without forward velocity, i.e., the vehicle is allowed to trim within a small range from neutral buoyancy in seawater [38]. In fact, due to the on-off type flowrate regulating mechanism, the vertical imbalanced force cannot be fully compensated by the VBS which will continuously work to counteract the left unbalanced effect, and this produces a small steady-state oscillation of hovering control of the vehicle, i.e., a limit cycle [18]. Despite this, satisfactory hovering performance is achieved as long as it meets the practical requirements of control accuracy.

Due to this fact, for the transition from hovering to cruising at the same depth, a trigger condition should be determined based on the following principles: (1) the left vertical unbalanced force must be in the scope of the fins authority so that it can be counteracted by the fins; (2) the absolute value of depth error should be less than a preset criteria for fast maintaining the cruising depth via fins.

The proposed state transition in Figure 3 from cruising at depth A to B, or vice versa, applies to when there is a large depth change, which takes long time, thus too much propulsion power consumption, for settling via the fins. For a small depth change, the transition can be done directly and quickly by fin control.

The advantages of the combined control strategy are that (1) vehicles can perform convenient diving/surfacing without propulsion via the energy-efficient, easily constructed and controlled on-off type VBS; (2) satisfactory and low-power hovering control can be achieved via the VBS, which effectively overcomes the absence or insufficiency of lift of the fins at zero or low speed; (3) the VBS can fulfill fast descending/ascending when there is a large change in the cruising depth, which will greatly shorten the transient period and thus reduce the propeller energy consumption; (4) the fins alone are actuated to counteract the remaining small vertical unbalanced force and maintain the desired depth, making cruising more energy-efficient.

#### 4. On-Off Type VBS and Fin Control Design

According to the proposed combined control strategy, the VBS and the fins do not work simultaneously. Hence, close-loop controller designs of the VBS and the fins are based on different control models simplified from system (2). This section gives the different control models and the on-off type VBS and the fin controllers are developed accordingly.

#### 4.1. On-Off Type VBS Control Design

By substituting  $\delta_b = \delta_s = 0$  into system (2), the depth control model via on-off type VBS is obtained

$$\begin{aligned}\dot{e}_z &= -w, \\ (m_0 + m_a - Z_w)\dot{w} &= (Z_w + Z_{w|w|}|w|)w + m_a g + Z_0, \\ \dot{m}_a &= q, m_a \in [0, \bar{m}_a] \text{ \& } q \in \{-\bar{q}, 0, \bar{q}\}\end{aligned}\quad (3)$$

The proposed hierarchical control scheme for the VBS, which is depicted in Figure 4, consists of a ballast mass planner (the upper layer) outputting the demanded dynamic ballast mass  $m_d$  to stabilize the heave motion, and a flowrate controller (the lower layer) generating the continuous mass flowrate  $q_c$  to achieve fast tracking of  $m_d$ .  $q_c$  is then quantized to generate the final on-off type flowrate command  $q$ . The actual ballast mass  $m_a$ , the depth  $z$ , the depth rate  $w$  and the depth acceleration  $\dot{w}$  are available directly or can be derived from a water level sensor, a pressure depth sensor, an acoustic doppler current profiler and an inertial navigation system.

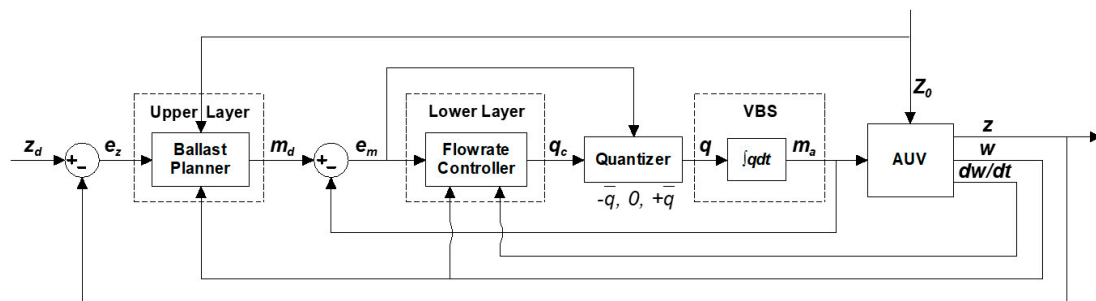


**Figure 4.** Hierarchical architecture-based control design of the VBS.

##### 4.1.1. Upper Layer Design

The upper layer is a ballast water mass planner which generates the demanded dynamic mass of ballast water to stabilize the heave motion of the vehicle. It combines a PD-type feedback control law with a feedforward control component, that is

$$\begin{aligned}m_d &= k_p e_z + k_d \dot{e}_z - g^{-1} Z_0 \\ &= k_p e_z - k_d w - g^{-1} Z_0,\end{aligned}\quad (4)$$

where  $k_p$  and  $k_d$  are the proportional and derivative gains, respectively, and the feedforward term  $-g^{-1} Z_0$  is included to compensate for the unbalanced gravity and buoyancy.

When the actual ballast water reaches the demanded value, i.e.,  $m_a = m_d$ , the theoretical analysis given below shows that with proper  $k_p$  and  $k_d$ , globally asymptotical stability of system (3) is guaranteed. To this end, replacing  $q$  with  $q_c$  and substituting  $m_a = k_p e_z - k_d w - g^{-1} Z_0$  into (3) yields

$$\begin{aligned}\dot{e}_z &= -w, \\ (m_0 + m_a - Z_w)\dot{w} &= (Z_w + Z_{w|w|}|w|)w + (k_p e_z - k_d w)g, \\ \dot{m}_a &= q_c, m_a \in [0, \bar{m}_a] \text{ \& } q_c \in [-\bar{q}, \bar{q}]\end{aligned}\quad (5)$$

A Lyapunov function is designed as follows, based on the kinetic and potential energy of system (5) [36]

$$V = \frac{1}{2} k_p g e_z^2 + \frac{1}{2} (m_0 + m_a - Z_w) w^2. \quad (6)$$

Taking the derivative of  $V$  with respect to  $t$  gives

$$\dot{V} = k_p g e_z \dot{e}_z + \frac{1}{2} \dot{m}_a w^2 + (m_0 + m_a - Z_{\dot{w}}) w \dot{w}. \quad (7)$$

Substituting (5) into (7) yields

$$\dot{V} = (Z_w + Z_{w|w|}|w|)w^2 + (q_c/2 - k_d g)w^2. \quad (8)$$

As the inertial term  $m_0 + m_a - Z_{\dot{w}}$  and the damping term  $Z_w + Z_{w|w|}|w|$  of an AUV are always positive and negative, respectively, (6) and (8) implies that  $V$  is positive definite and

$$\dot{V} \leq (Z_w + Z_{w|w|}|w|)w^2 \leq 0, \quad (9)$$

for any  $e_z$  and  $w$  when choosing  $k_p > 0$  and  $k_d > \bar{q}/(2g)$ .

Moreover,  $\dot{V} = 0$  implies  $w = 0$ , in terms of which it can be obtained from (5) that

$$\dot{w} = \frac{k_p g e_z}{m_0 + m_a - Z_{\dot{w}}}. \quad (10)$$

Therefore,  $\dot{w}$  will be non-zero if  $e_z \neq 0$  and  $\dot{V} = 0$  only if  $e_z = 0$ . This means that when  $m_a$  tracks and reaches  $m_d$  by proper design of  $q_c$ , system (3) will not get stuck and global asymptotic stability can be achieved with  $k_p > 0$  and  $k_d > \bar{q}/(2g)$ .

#### 4.1.2. Lower Layer Design

Based on the above analysis, a continuous flowrate algorithm should be designed to achieve fast and accurate tracking of the upper layer output. To achieve this goal, denote the mass tracking error as

$$e_m = m_d - m_a, \quad (11)$$

and let

$$\dot{e}_m = -\alpha \cdot \text{sign}(e_m), \quad (12)$$

where  $\alpha > 0$  is a constant parameter to be designed. Obviously,  $e_m$  will approach zero in finite time.

Combining (5), (11) and (12), the continuous mass flowrate algorithm is obtained

$$q_c = \alpha \cdot \text{sign}(e_m) - k_p w - k_d \dot{w}. \quad (13)$$

#### 4.1.3. Quantization Principle for Generating the On-Off Flowrate Command

In this section, the continuous mass flowrate  $q_c$ , which assures fast and accurate tracking of the demand dynamic ballast mass, is quantized based on the following principle to generate on-off flowrate command for the on-off type VBS.

Firstly, the continuous flowrate law (13) is refined as follows to reduce chattering of the flow control valves around small mass tracking errors

$$q_c = \begin{cases} \alpha \cdot \text{sign}(e_m) - k_p w - k_d \dot{w}, & |e_m| > \bar{e}_m \\ -k_p w - k_d \dot{w}, & |e_m| \leq \bar{e}_m \end{cases}, \quad (14)$$

where  $\bar{e}_m$  denotes the thickness of the boundary layer of the mass tracking error.

The on-off type flowrate command  $q$  is then generated via quantization of  $q_c$  based on the threshold of half of the constant flowrate of the on-off type VBS.

$$q = \begin{cases} \bar{q} \cdot \text{sign}(q_c), & |q_c| > \bar{q}/2 \\ 0, & |q_c| \leq \bar{q}/2 \end{cases}. \quad (15)$$

Note that although the continuous mass flowrate algorithm  $q_c$  is expected to guarantee the precise mass tracking of the ballast planner and the vehicle finally reaches static equilibrium, the quantized on-off type  $q$  will always result in a small and dynamic mass tracking error  $e_m$  practically. Thus, the VBS will keep working to compensate for the remaining vertical unbalanced force, and this produces a slight oscillation around the desired depth.

Despite this, both the ballast mass tracking and the depth control performance of the proposed on-off type flowrate command (15) are verified via simulations and basin tests in Section 5.

#### 4.2. Fin Control Design

According to the proposed combined control strategy and the above analysis, the fin controller takes effect for cruising after the vehicle is quasi-stabilized by the on-off type VBS system, which indicates that a quasi-static vertical equilibrium of the vehicle is achieved, i.e.,  $m_a g + Z_0 = -e_m^* g$ , where  $e_m^*$  is a small unknown constant mass tracking error due to the on-off type flowrate regulating mechanism, and should be in the scope of fins authority. Substituting this into system (2), the depth control model via fins is obtained

$$\begin{aligned} \dot{e}_z &= -w, \\ (m_0 + m_a - Z_w)\dot{w} &= (Z_w + Z_{w|w|}|w|)w + Z_{\delta_b}\delta_b + Z_{\delta_s}\delta_s - e_m^* g. \end{aligned} \quad (16)$$

Denote the total lift of the bow and stern fins as  $Z_\delta = Z_{\delta_b}\delta_b + Z_{\delta_s}\delta_s$ , and the arm lengths of the bow and stern fins as  $l_{\delta_b}$  and  $l_{\delta_s}$ , respectively. Choose a PD-control law for  $Z_\delta$

$$Z_\delta = k_p^* e_z + k_d^* \dot{e}_z = k_p^* e_z - k_d^* w, \quad (17)$$

where  $k_p^*$  and  $k_d^*$  are the proportional and derivative gains of the fin controller, respectively.

Let  $z_d^* = z_d - e_m^* g/k_p^*$  and define  $e_z^* = z_d^* - z$ , then the fin control system can be expressed as

$$\begin{aligned} \dot{e}_z^* &= -w, \\ (m_0 + m_a - Z_w)\dot{w} &= (Z_w + Z_{w|w|}|w|)w + k_p^* e_z^* - k_d^* w. \end{aligned} \quad (18)$$

Similarly, in the same way as Section 4.1.1, the vehicle can be proved to achieve global asymptotic stability and converge to the steady state  $z_d^*$ , which has an offset of  $e_m^* g/k_p^*$  deviated from the desired value, under the control law (17) with  $k_p^* > 0$  and  $k_d^* > 0$  when choosing Lyapunov function as  $V = \frac{1}{2}k_p^* e_z^{*2} + \frac{1}{2}(m_0 + m_a - Z_w)w^2$ .

That is, the remaining small unbalanced force  $-e_m^* g$  caused by the on-off type VBS is totally counteracted by the fins and the vehicle will cruise at the depth  $z_d^*$  with a steady-state error of  $e_{ss} = e_m^* g/k_p^*$ .  $e_{ss}$  can be reduced, to a certain extent, by choosing a smaller  $\bar{e}_m$  on one hand to improve the precision of mass tracking, which, however, will increase the chattering phenomenon of the valves, and an appropriately larger  $k_p^*$  on the other hand. It is common to choose a larger  $\bar{e}_m$  and a proper  $k_p^*$  as long as it meets the practically required control accuracy.

To result in zero pitch torque of the bow and stern fins, the following equation is satisfied

$$Z_{\delta_b}\delta_b l_{\delta_b} - Z_{\delta_s}\delta_s l_{\delta_s} = 0. \quad (19)$$

Combining (17) and (19), the control inputs of the fin controller are obtained

$$\delta_b = \frac{l_{\delta_s}(k_p^* e_z - k_d^* w)}{(l_{\delta_b} + l_{\delta_s})Z_{\delta_b}}, \delta_s = \frac{l_{\delta_b}(k_p^* e_z - k_d^* w)}{(l_{\delta_b} + l_{\delta_s})Z_{\delta_s}}. \quad (20)$$

Note that the bow and stern fins can be used for depth and pitch control simultaneously. In this work, the AUV is designed with strong passive pitch stability which can be observed in the results of basin tests. Thus, only depth control via fins is considered.

## 5. Validation Results and Discussion

Simulation as well as basin test validations were conducted on a middle-sized AUV with a length and a maximal diameter of about 4 and 0.5 m, respectively, to assess the mass tracking and hovering performance of the developed on-off type VBS control system, and the depth control performance of the proposed combined control strategy. The AUV was designed and constructed by the State Key Laboratory of Ocean Engineering, Shanghai Jiao Tong University. Simulations were conducted in the MATLAB/Simulink environment, and experiments were carried out in the ocean engineering basin of the State Key Laboratory of Ocean Engineering, Shanghai Jiao Tong University.



The vehicle was equipped with a one-tank on-off type VBS. The physical parameters included  $m_0 = 367$  kg,  $\bar{m}_a = 5$  kg and  $\bar{q} = 0.04$  kg/s. The CFD computed hydrodynamic coefficients were  $Z_w = -481.60$  kg,  $Z_{\dot{w}} = -6.00$  kg/s and  $Z_{w|w|} = -396.00$  kg/m. The required depth control accuracy in this work is not worse than  $\pm 0.05$  m, i.e.,  $\bar{e}_z = 0.05$  m.

### 5.1. Simulation Validation

A comparative study on the mass tracking and the hovering performance of the proposed on-off and the continuous flowrate control is conducted.

Assume the vehicle has a net buoyancy of 1.35 kg when the ballast tank is empty, i.e.,  $Z_0 = -13.23$  N, and initially hovers at a certain depth, which means  $m_a(0)g + Z_0 = 0$  or  $m_a(0) = 1.35$  kg, and is commanded to response to a depth change demand of 1 m. The controller parameters are determined as  $\alpha = 0.12$ ,  $k_p = 1.14$  and  $k_d = 18$ . The thickness of the boundary layer of the mass tracking error is chosen as  $\bar{e}_m = 0.01$  kg. The simulation results are shown in Figures 5–9.

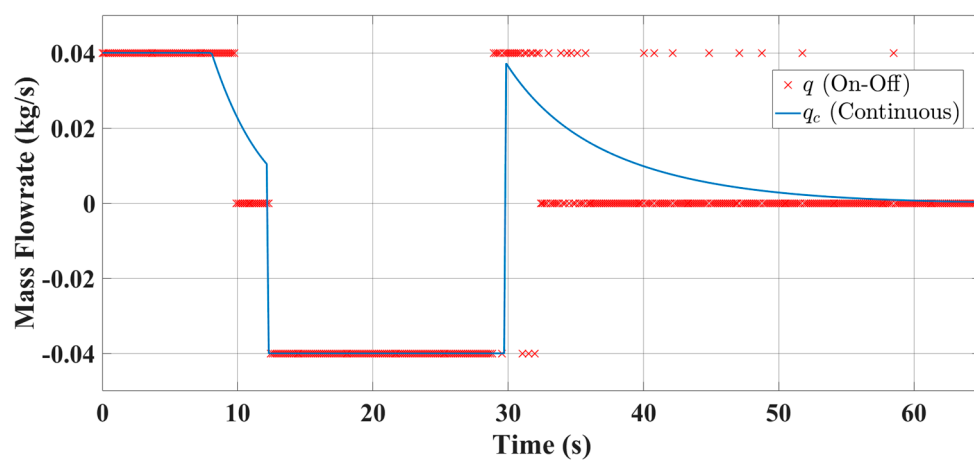


Figure 5. Mass flowrates of on-off and continuous type VBS control.

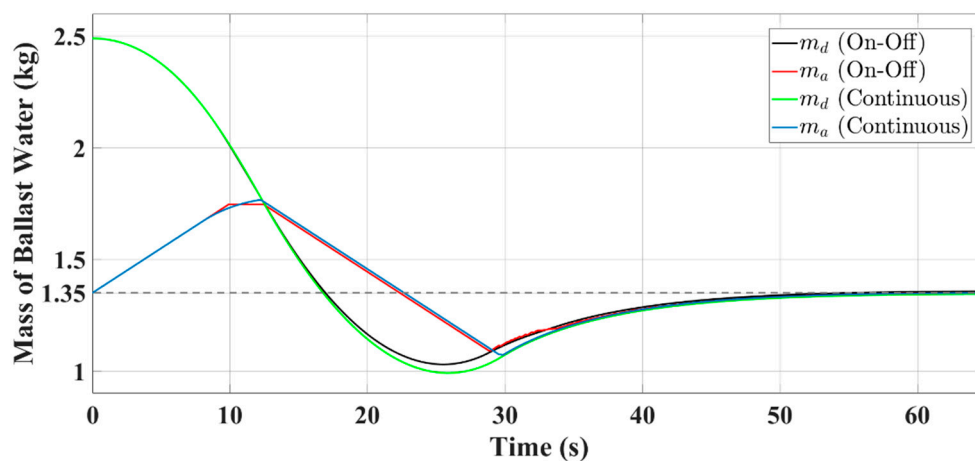


Figure 6. Demanded and actual ballast mass changes of on-off and continuous type VBS control.

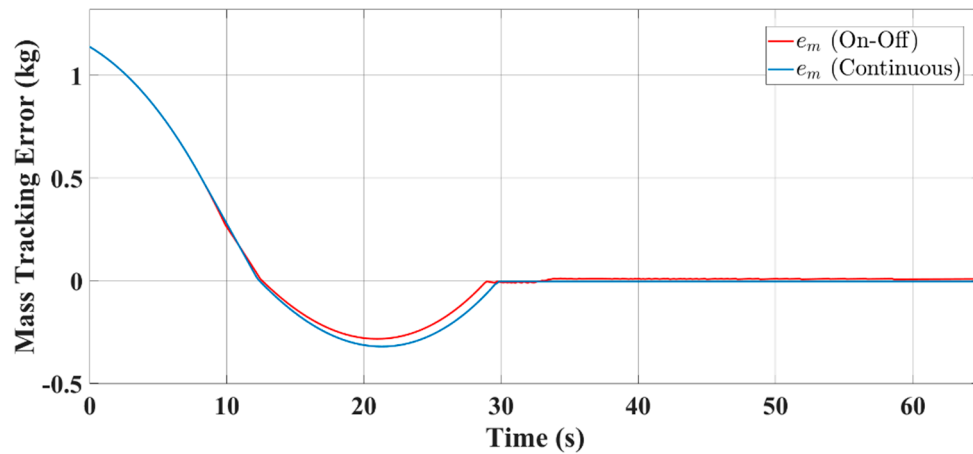


Figure 7. Ballast mass tracking errors of on-off and continuous type VBS control.

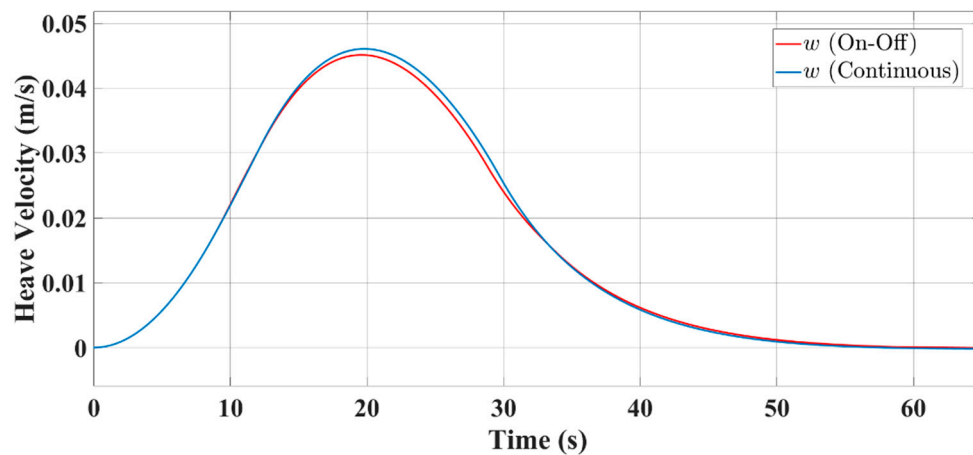


Figure 8. Heave velocity responses of on-off and continuous type VBS control.

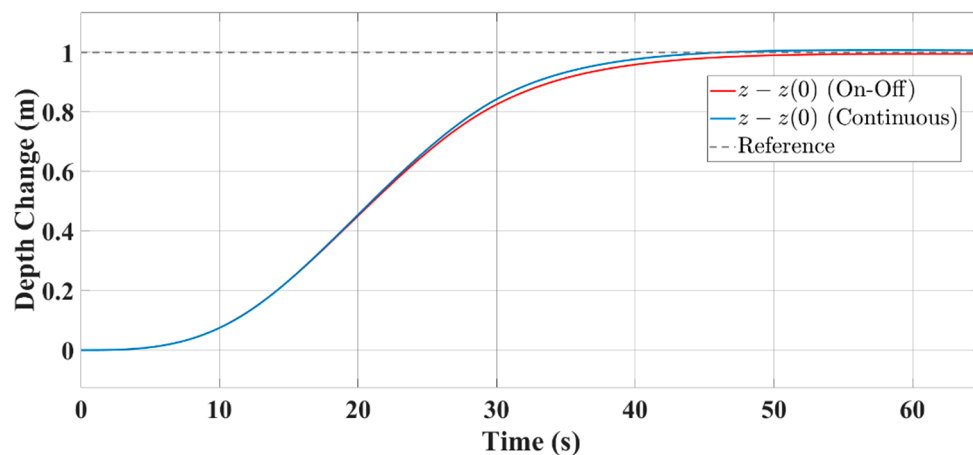


Figure 9. Depth change responses of on-off and continuous type VBS control.

The mass flowrates of the on-off and the continuous VBS control are given in Figure 5. The detailed mass tracking performances can be observed in Figures 6 and 7, which indicate that the actual masses of ballast water of both on-off and continuous type have a quick and satisfying tracking to their respective demanded values, and finally reach an agreement to counteract the imbalanced force  $Z_0$ . The responses of heave motion states shown in Figures 8 and 9 obviously demonstrate that the proposed on-off type flowrate control exhibits about equally desirable hovering performance as

the continuous one. Both of the absolute depth errors are less than 0.01 m, assuring the required control accuracy.

It should be pointed out that negligible depth error can be observed in the on-off type control from Figure 9. As explained in Section 4.1.3, this is because accurate mass tracking cannot be achieved under the refined and quantized on-off flowrate law (15). Thus, the vehicle is finally in a quasi-static vertical equilibrium, and the VBS continuously works to counteract the small unbalanced force. This produces a negligible steady-state oscillation of the vehicle hovering, which can be seen if the simulation lasts long enough. Although the depth error could be reduced, to a certain extent, by choosing a smaller  $\bar{e}_m$  to improve the precision of mass tracking, it is common to choose a larger  $\bar{e}_m$  as long as it meets the practical requirements of control accuracy.

## 5.2. Basin Test Validation

Basin tests, which comprise two parts—hovering control via the on-off type VBS and depth control under the combined strategy—were carried out for further verification of the proposed on-off type VBS hovering control system and the combined depth control strategy.

### 5.2.1. Hovering Control via On-Off Type VBS

The vehicle has a net buoyancy of 1.35 kg with the ballast tank empty. It is required to dive from the water surface to the depth of 1.5 m with 1.17 kg of ballast water already in the tank. The parameters of the VBS controller are determined as  $\alpha = 0.04$ ,  $k_p = 0.25$  and  $k_d = 5$ . The thickness of the boundary layer of the mass tracking error is chosen as  $\bar{e}_m = 0.01$  kg.

The experimental results are presented in Figures 10–13, from which it can be seen that the dynamic mass tracking error is within  $\pm 0.01$  kg and the absolute depth error is not worse than 0.01 m after settling. Both the mass tracking and the hovering control performance are well guaranteed under the proposed on-off flowrate control.

Figure 14 shows the hovering ability of the VBS depth controller of the Seahorse AUV in [18]. It is plotted from an in-water test with a depth command of 2 m from the water surface. Although the vehicle finally hovers near the commanded depth, the hovering performance can be improved.

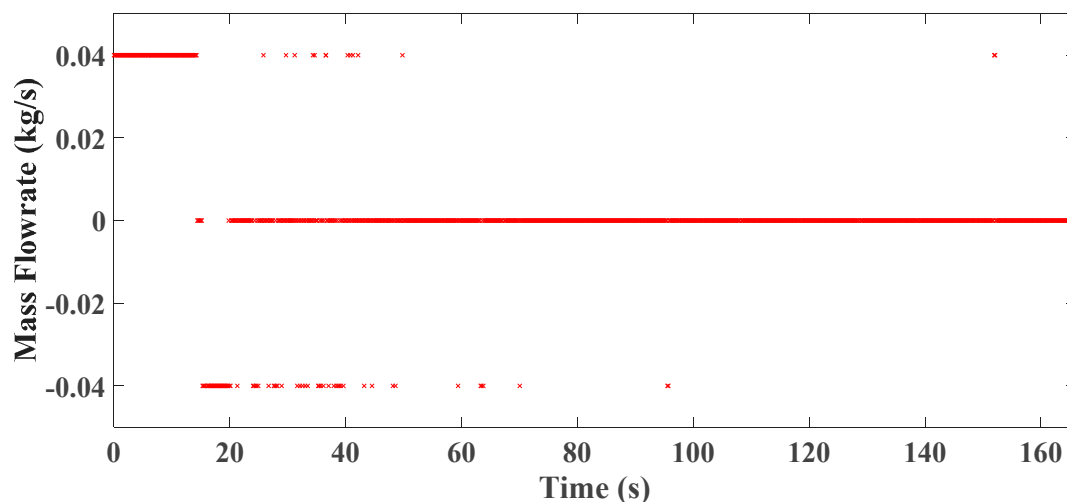


Figure 10. Mass flowrate of hovering control via on-off type VBS.

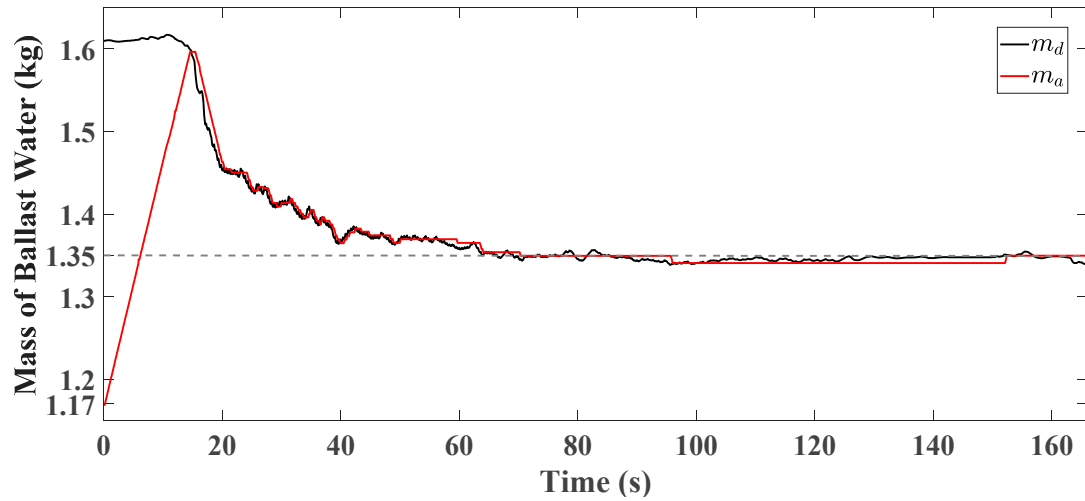


Figure 11. Demanded and actual ballast mass changes of hovering control via on-off type VBS.

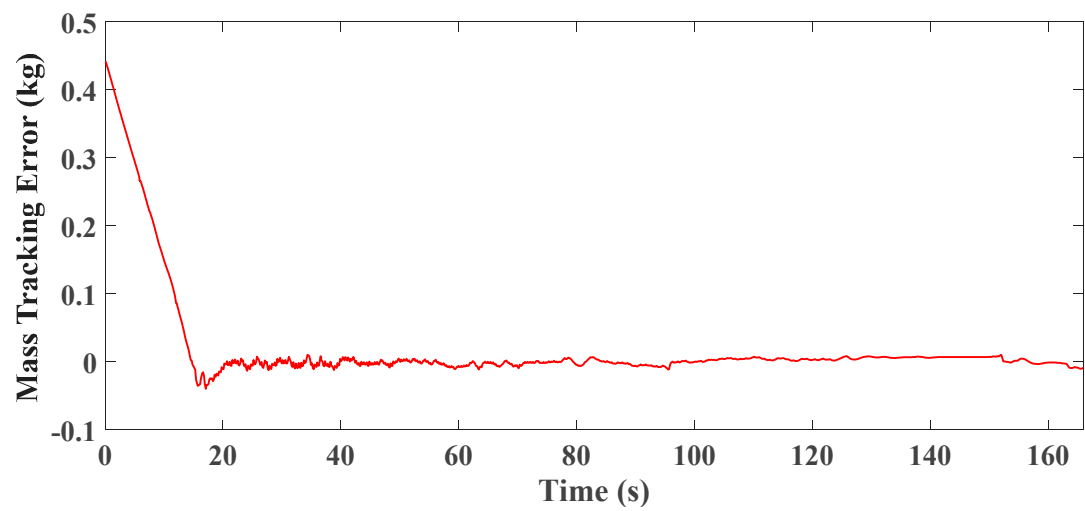


Figure 12. Ballast mass tracking error of hovering control via on-off type VBS.

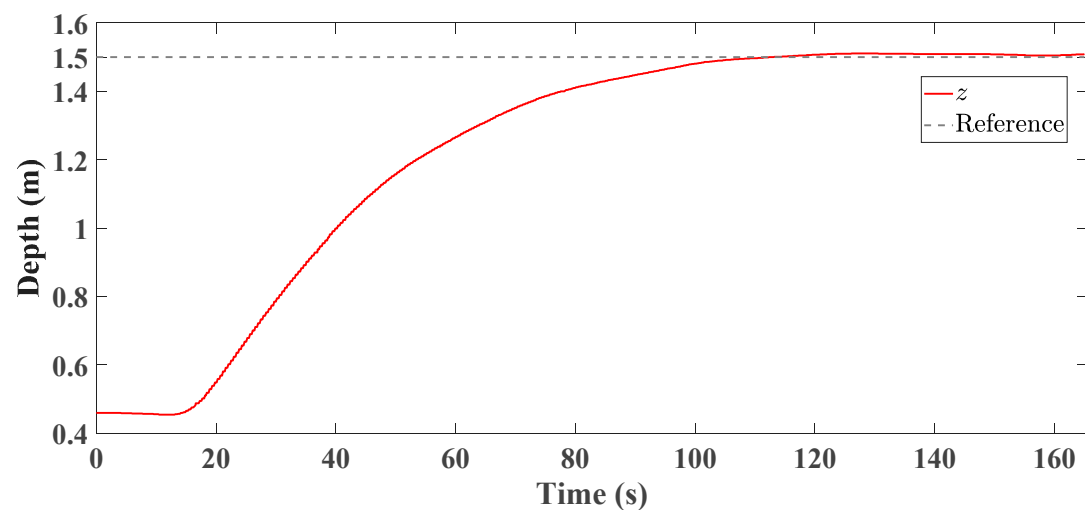
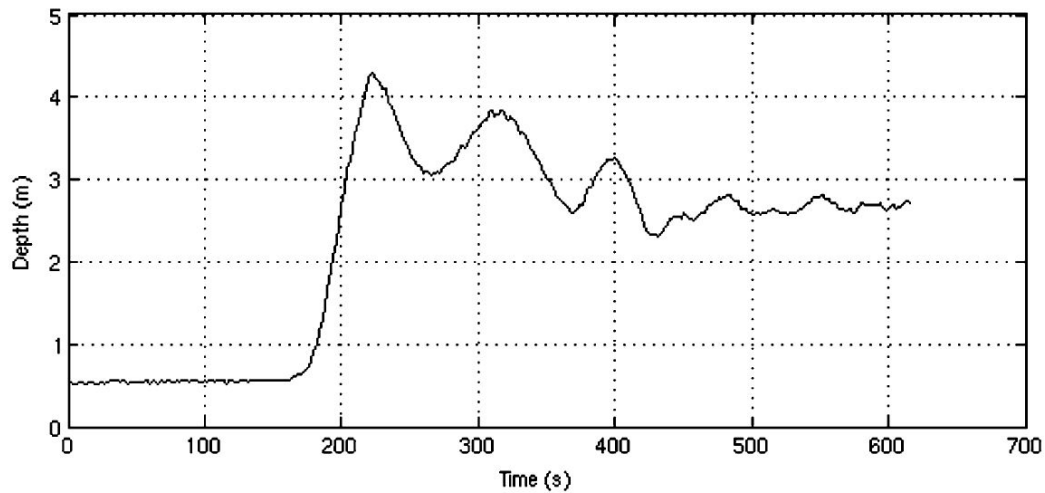


Figure 13. Depth response of hovering control via on-off type VBS.



**Figure 14.** Depth response of hovering control via on-off type VBS of Seahorse AUV in [18], with the permission from IEEE, 2007.

### 5.2.2. Depth Control under Combined Control Strategy

To validate the combined depth control strategy, the vehicle is commanded to launch from the surface and dive to the depth of 1.2 m via the on-off type VBS. Then, the VBS is stopped and the propelling system, as well as the fins and rudders, are triggered to work concurrently. The forward velocity is kept at a constant 0.17 m/s via the control of the propeller, and the heading angle is set as zero via the control of the stern rudders. The bow and stern fins work together at such operating conditions to counteract the small unbalanced force and maintain the cruising depth of 1.2 m.

The vehicle has a net buoyancy of 1.50 kg with an empty ballast tank. It is initially on the water surface with 1.37 kg of ballast water already in the tank. The lift coefficients of the bow and stern fins, at the constant forward velocity of 0.17 m/s, are  $Z_{\delta_b} = Z_{\delta_s} = 0.1$  N/deg. And the fins are designed to have the same arm lengths, i.e.,  $l_{\delta_b}/l_{\delta_s} = 1$ . Thus, the deflection commands of the bow and stern fins are always the same according to (20), and they are uniformly denoted by  $\delta$ .  $\delta$  is limited in the range of  $-20$  to  $20$  deg as the fins have the best effect at  $\pm 20$  deg for the forward velocity of 0.17 m/s. The parameters of the fin controller are chosen as  $k_p^* = 500$  and  $k_d^* = 1120$ . The experimental results are depicted in Figures 15–20.

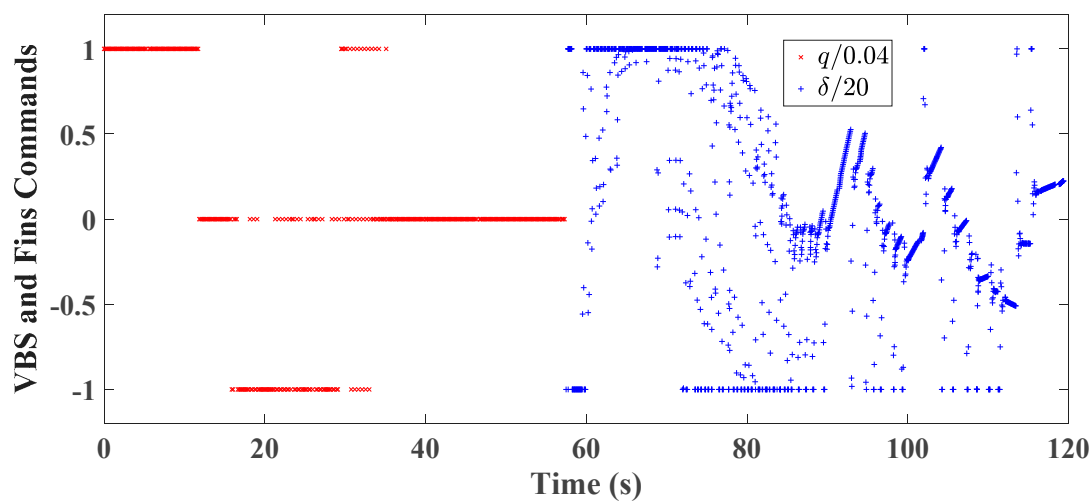


**Figure 15.** Normalized VBS and fins commands of depth control under combined control strategy.

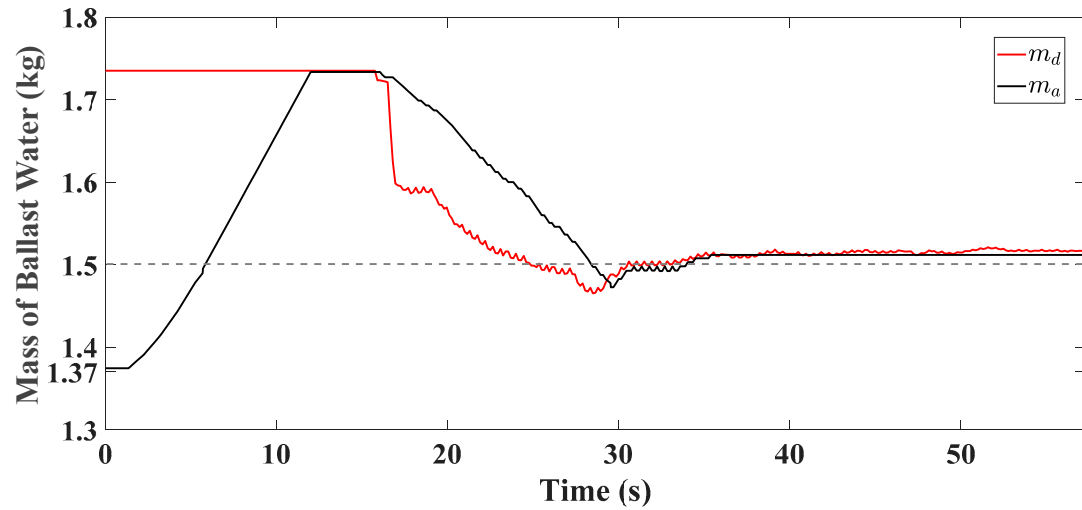


Figure 16. Demanded and actual ballast mass changes of depth control via on-off type VBS.

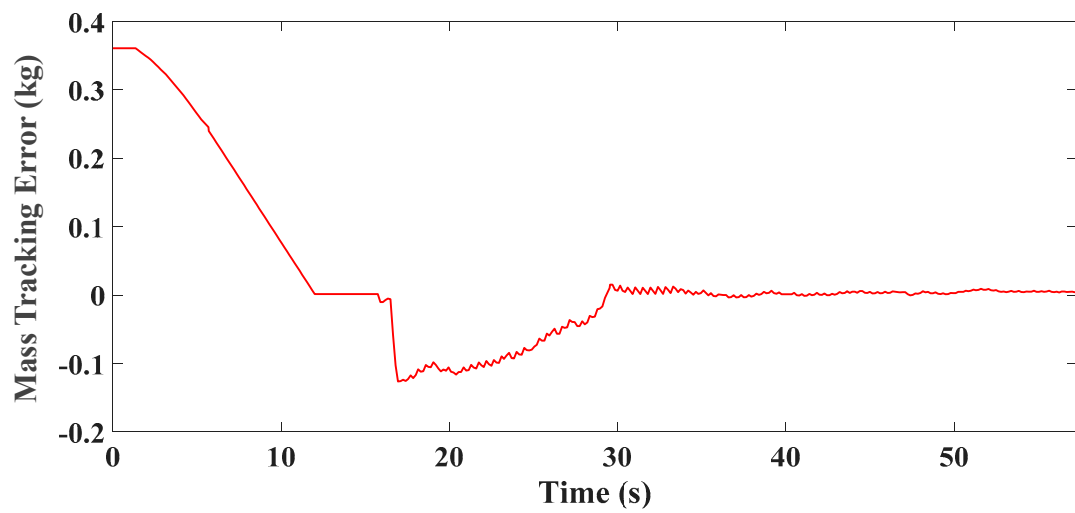


Figure 17. Ballast mass tracking error of depth control via on-off type VBS.

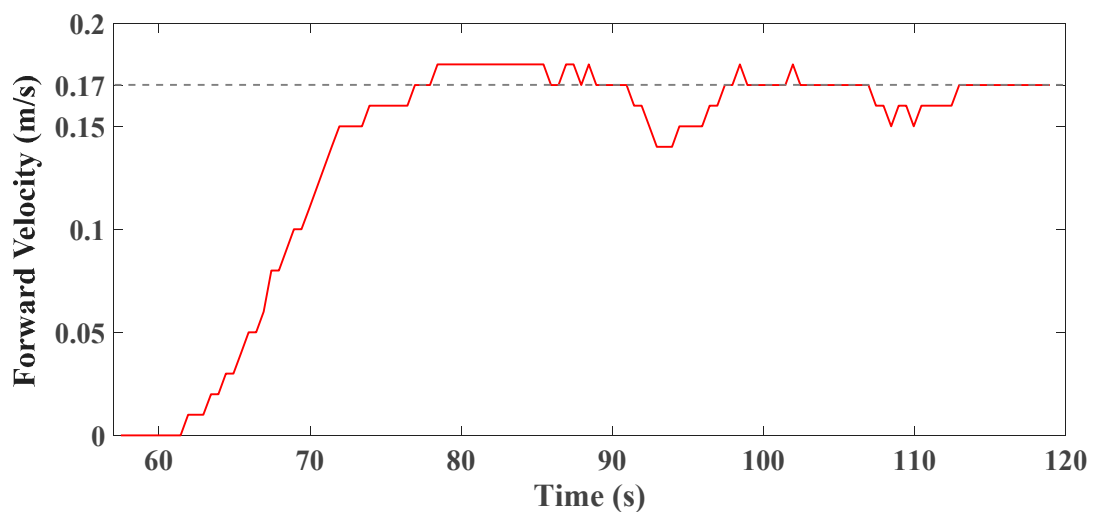


Figure 18. Forward velocity response at the stage of fins control.

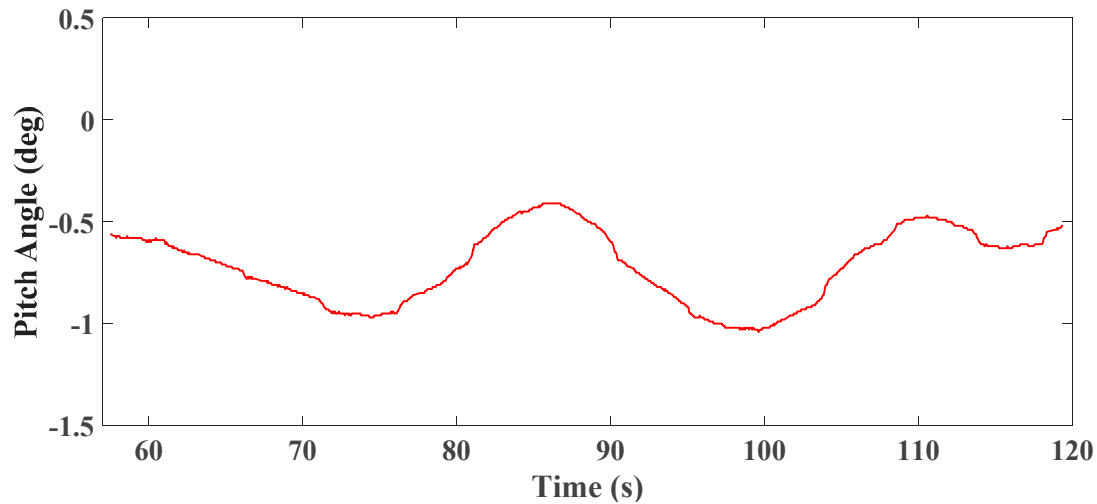


Figure 19. Pitch angle response of the vehicle at the stage of fins control.

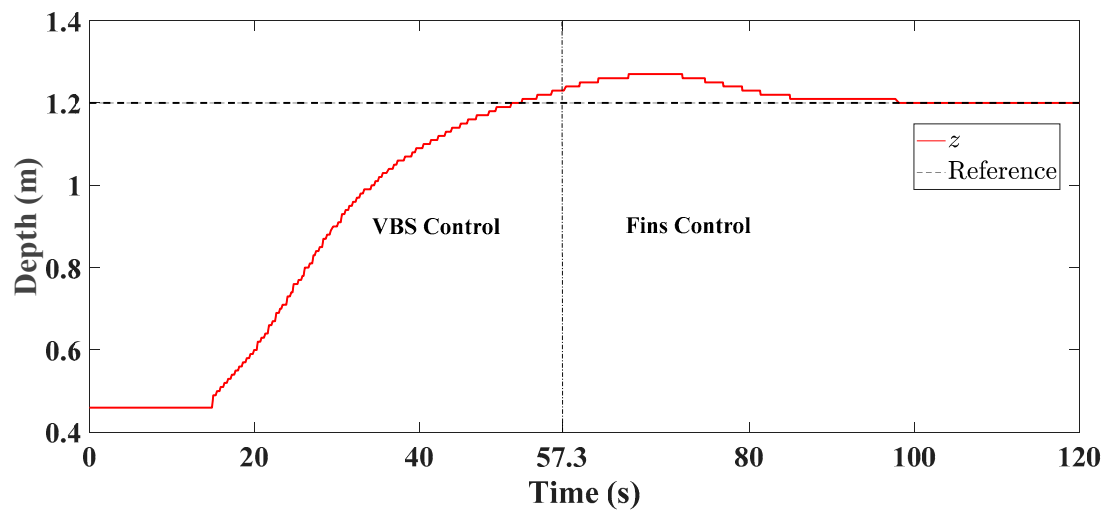


Figure 20. Depth response under combined control strategy.

The normalized VBS and fin commands are given in Figure 15 chronologically. Figures 16 and 17 reveal the good mass tracking performance of the on-off type VBS again, despite the inherent small tracking error. The forward velocity response is depicted in Figure 18, which shows that the vehicle reaches the velocity of 0.05 m/s, at which the fins come into play, at about  $t = 65$  s. The pitch angle response seen in Figure 19 shows the good passive pitch stability of the vehicle. The satisfactory depth control performance of the combined control strategy is verified in Figure 20. It shows that the VBS stops and the fins start working at  $t = 57.3$  s and the vehicle continues descending, due to inertia, to the maximum depth of 1.27 m at about  $t = 65$  s. It is at this moment that the fins take effect, and the depth is restored and well maintained with almost no steady-state error.

### 5.3. Hovering Control Performance under Model Uncertainty and Unknown Disturbances

The above work assumes that AUVs operate under nominal conditions, i.e., without modeling errors and external disturbances. As the precise estimation of the hydrodynamic coefficients is difficult, and unknown disturbance cannot be neglected when working under rough sea conditions, the behaviors of the proposed hovering control system with respect to such nuisances are further studied via simulations. The vehicle is assumed to have a net buoyancy of 1.35 kg when the ballast tank is empty and initially hovers at a certain depth, and is commanded to respond to a depth change demand of 1 m.

### 5.3.1. Hovering Control under Modeling Errors

Study of the proposed scheme for systems with different levels of modeling errors is done with the results presented in Figure 21.  $\hat{Z}_w = (1 + \delta)Z_w$ ,  $\hat{Z}_w = (1 + \delta)Z_w$  and  $\hat{Z}_{w|w|} = (1 + \delta)Z_{w|w|}$  are used in the simulations instead of their nominal counterparts, where  $\delta (> -1)$  is applied to describe the degree of modeling errors.

As is shown in Figure 21, the robustness of the proposed method to system modeling errors is still guaranteed, despite the degradation of hovering performance with bigger overshoot (as  $\delta$  is positive and increases) or longer settling time (as  $\delta$  is negative and decreases).

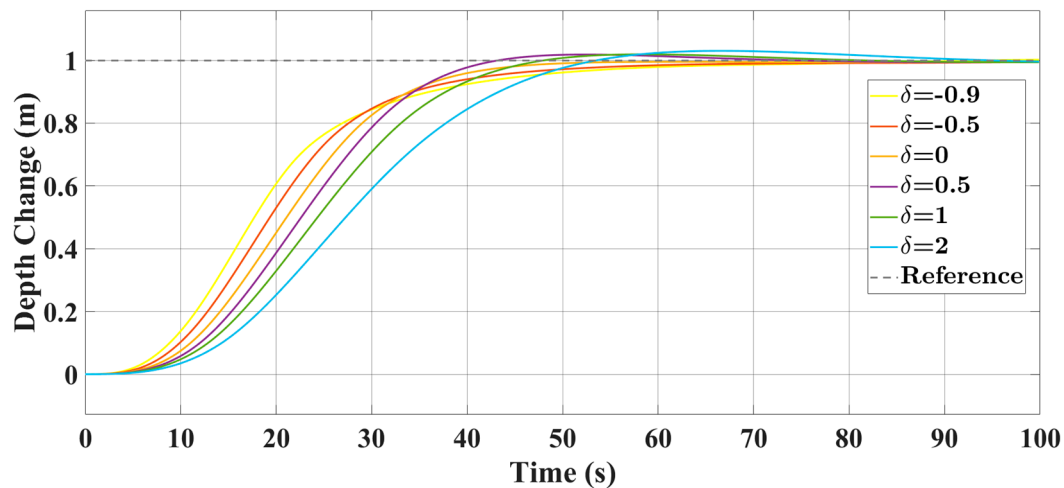


**Figure 21.** Hovering control responses under different levels of modeling errors.

### 5.3.2. Hovering Control under External Disturbance

In this case, constant external disturbances of  $d = 2 \text{ N}$  and  $d = -2 \text{ N}$  are considered. The results in Figure 22 show that steady state errors occur due to the unknown disturbances. For practical underwater missions, seawave or current disturbances which may be time-varying cannot be neglected. Thus, it is our future work to combine anti-disturbance strategies with the proposed hovering control scheme.

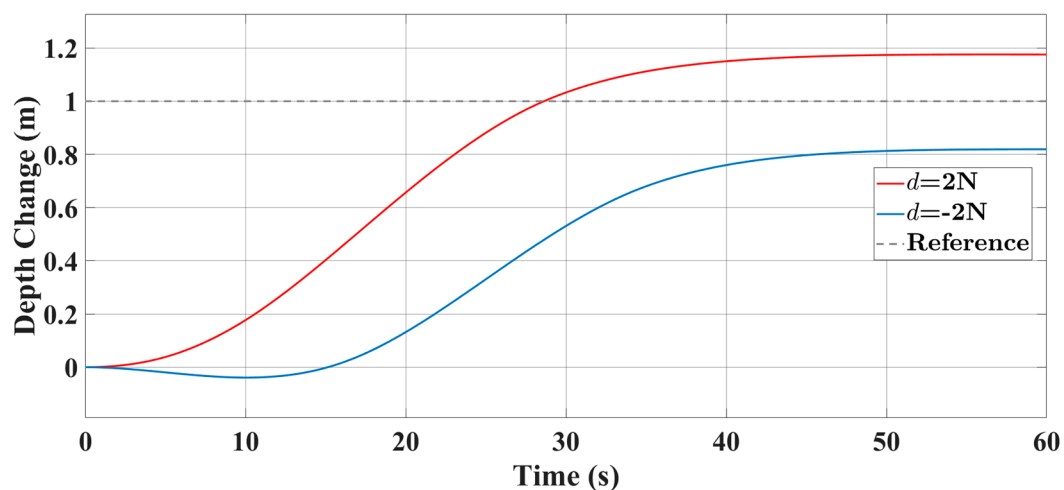


**Figure 22.** Hovering control responses under external disturbances.

## 6. Conclusions

In this paper, a combined depth control strategy is proposed to enable hovering and low-speed and long-range cruising capabilities for AUVs. To achieve this goal, bow and stern fins are adopted



in combination with an on-off type VBS. The VBS affords the capabilities of satisfactory and low-power hovering, and fast descending/ascending to reach the designated cruising depth, which will greatly shorten the transient period and thus reduce the propeller energy consumption. The fins alone are actuated to counteract the remaining small vertical unbalanced force due to the on-off type flowrate regulating mechanism and maintain the desired depth, making cruising more energy efficient. A hierarchical architecture-based on-off type flowrate controller is developed for the VBS to assure satisfactory hovering performance. Numerical and experimental studies demonstrate the effectiveness of the on-off type VBS controller and the combined depth control strategy.

Further studies are conducted showing that the on-off type VBS hovering system is robust to model uncertainty. However, steady state error occurs under external disturbance, which cannot be neglected for underwater applications under seawave and current conditions. Anti-disturbance strategies will be investigated in future works.

**Author Contributions:** conceptualization, A.B.; methodology, A.B.; software, A.B.; validation, A.B.; formal analysis, A.B.; writing—original draft preparation, A.B.; writing—review and editing, A.B. and X.Z.; visualization, A.B. and F.Z.; supervision, T.G. All authors have read and agreed to the published version of the manuscript.

**Funding:** This research received no external funding.

**Conflicts of Interest:** The authors declare no conflict of interest.

## References

1. Fletcher, B.; Bowen, A.; Yoerger, D.R.; Whitcomb, L.L. Journey to the challenger deep: 50 years later with the Nereus hybrid remotely operated vehicle. *Mar. Technol. Soc. J.* **2009**, *43*, 65–76, doi:10.4031/MTSJ.43.5.26.
2. Galceran, E.; Campos, R.; Palomeras, N.; Ribas, D.; Carreras, M.; Ridao, P. Coverage path planning with real-time replanning and surface reconstruction for inspection of three-dimensional underwater structures using autonomous underwater vehicles. *J. Field Robot.* **2015**, *32*, 952–983, doi:10.1002/rob.21554.
3. Gao, X.; Ding, K.; Ren, Y.G.; Fu, W.T.; Ding, Z.J.; Zhao, S.Y.; Liu, B.H. Target deployment and retrieval using JIAOLONG manned submersible in the depth of 6600 m in Mariana Trench. *China Ocean Eng.* **2017**, *31*, 618–623, doi:10.1007/s13344-017-0071-9.
4. Kaminski, C.; Crees, T.; Ferguson, J.; Forrest, A.; Williams, J.; Hopkin, D.; Heard, G. 12 days under ice—an historic AUV deployment in the Canadian High Arctic. In Proceedings of the 2010 IEEE/OES Autonomous Underwater Vehicles (AUV), Monterey, CA, USA, 1–3 September, 2010; pp. 1–11, doi:10.1109/AUV.2010.5779651.
5. Khojasteh, D.; Kamali, R. Design and dynamic study of a ROV with application to oil and gas industries of Persian Gulf. *Ocean Eng.* **2017**, *136*, 18–30, doi:10.1016/j.oceaneng.2017.03.014.
6. Maurya, P.K.; de Sa, E.; Dubey, A.C.; Dabholkar, N.; Pascoal, A. Autonomous hovering profiler. In Proceedings of the 2016 IEEE/OES Autonomous Underwater Vehicles (AUV), Univ Tokyo, Inst Ind Sci, Tokyo, Japan, 6–9 November, 2016; pp. 268–272, doi:10.1109/AUV.2016.7778682.
7. Omerdic, E.; Toal, D.; Nolan, S.; Ahmad, H.; Duffy, G. Design & development of assistive tools for future applications in the field of renewable ocean energy. In Proceedings of the OCEANS 2011 IEEE-Spain, Santander, SPAIN, 6–9 June 2011; pp. 1–6, doi:10.1109/Oceans-Spain.2011.6003454.
8. Qiu, C.H.; Mao, H.B.; Wang, Y.H.; Yu, J.C.; Su, D.Y.; Lian, S.M. An irregularly shaped warm eddy observed by Chinese underwater gliders. *J. Oceanogr.* **2019**, *75*, 139–148, doi:10.1007/s10872-018-0490-0.
9. Singh, Y.; Bhattacharyya, S.K.; Idichandy, V.G. CFD approach to modelling, hydrodynamic analysis and motion characteristics of a laboratory underwater glider with experimental results. *J. Ocean Eng. Sci.* **2017**, *2*, 90–119, doi:10.1016/j.joes.2017.03.003.
10. Sorbi, L.; Scaradozzi, D.; Zoppini, F.; Zingaretti, S.; Gambogi, P. Robotic tools and techniques for improving research in an underwater delicate environment. *Mar. Technol. Soc. J.* **2015**, *49*, 6–17, doi:10.4031/MTSJ.49.5.5.
11. Xu, Z.Z.; Li, L.; Yu, J.C.; Xu, X.J.; Jia, M.F. A marine environment early warning algorithm based on marine data sampled by multiple underwater gliders. *China Ocean Eng.* **2019**, *33*, 172–184, doi:10.1007/s13344-019-0017-5.

12. Zapata-Ramírez, P.A.; Huete-Stauffer, C.; Scaradozzi, D.; Marconi, M.; Cerrano, C. Testing methods to support management decisions in coralligenous and cave environments. A case study at Portofino MPA. *Mar. Environ. Res.* **2016**, *118*, 45–56, doi:10.1016/j.marenvres.2016.04.010.
13. Zhao, X.; Liu, Y.; Han, M.; Wu, D.; Li, D. Improving the performance of an AUV hovering system by introducing low-cost flow rate control into water hydraulic variable ballast system. *Ocean Eng.* **2016**, *125*, 155–169, doi:10.1016/j.oceaneng.2016.08.001.
14. Gupta, S.; Hare, J.; Zhou, S. Cooperative coverage using autonomous underwater vehicles in unknown environments. In Proceedings of the MTS/IEEE Oceans Conference, Hampton Roads, VA, USA, 14–19 October 2012; pp. 1–5, doi:10.1109/OCEANS.2012.6405115.
15. Pyo, J.; Cho, H.; Joe, H.; Ura, T.; Yu, S.C. Development of hovering type AUV “Cyclops” and its performance evaluation using image mosaicing. *Ocean Eng.* **2015**, *109*, 517–530, doi:10.1016/j.oceaneng.2015.09.023.
16. Maki, T.; Ura, T.; Sakamaki, T. AUV navigation around jacket structures II: Map based path-planning and guidance. *J. Mar. Sci. Technol.* **2012**, *17*, 523–531, doi:10.1007/s00773-012-0183-0.
17. Li, J.H.; Lee, P.M. Design of an adaptive nonlinear controller for depth control of an autonomous underwater vehicle. *Ocean Eng.* **2005**, *32*, 2165–2181, doi:10.1016/j.oceaneng.2005.02.012.
18. Tangirala, S.; Dzielski, J. A variable buoyancy control system for a large AUV. *IEEE J. Ocean. Eng.* **2007**, *32*, 762–771, doi:10.1109/JOE.2007.911596.
19. Caccia, M.; Veruggio, G. Guidance and control of a reconfigurable unmanned underwater vehicle. *Control Eng. Practice* **2000**, *8*, 21–37, doi:10.1016/S0967-0661(99)00125-2.
20. Vasilescu, I.; Detweiler, C.; Doniec, M.; Gurdan, D.; Sosnowski, S.; Stumpf, J.; Rus, D. Amour v: A hovering energy efficient underwater robot capable of dynamic payloads. *Int. J. Robot. Res.* **2010**, *29*, 547–570, doi:10.1177/0278364909358275.
21. Kobayashi, R.; Okada, S. Development of hovering control system for an underwater vehicle to perform core internal inspections. *J. Nucl. Sci. Technol.* **2016**, *53*, 566–573, doi:10.1080/00223131.2015.1064331.
22. McFarland, D.; Gilhespy, I.; Honary, E. DIVEBOT: A diving robot with a whale-like buoyancy mechanism. *Robotica* **2003**, *21*, 385–398, doi:10.1017/S026357470300496X.
23. Medvedev, A.V.; Kostenko, V.V.; Tolstonogov, A.Y. Depth control methods of variable buoyancy AUV. In Proceedings of the 2017 IEEE OES International Symposium on Underwater Technology (UT), Busan, South Korea, 21–24 February 2017; doi:10.1109/UT.2017.7890333.
24. Singh, Y.; Polvara, R.; Sharma, S.; Hatton, D.C.; Sutton, R.; Wan, J. Design of a variable buoyancy engine for small scale underwater vehicle. In Proceedings of the International conference on advances in subsea engineering, structures and systems (ASESS 2016), 6–7 June, 2016; pp. 100–103 (4).
25. Font, R.; García-Peláez, J. On a submarine hovering system based on blowing and venting of ballast tanks. *Ocean Eng.* **2013**, *72*, 441–447, doi:10.1016/j.oceaneng.2013.07.021.
26. Woods, S.A.; Bauer, R.J.; Seto, M.L. Automated ballast tank control system for autonomous underwater vehicles. *IEEE J. Ocean. Eng.* **2012**, *37*, 727–739, doi:10.1109/JOE.2012.2205313.
27. Murphy, A.J.; Haroutunian, M. Using bio-inspiration to improve capabilities of underwater vehicles. In Proceedings of the 17th International Unmanned Untethered Submersible Technology Conference, Portsmouth, NH, USA, 21–24 August 2011; pp. 20–31.
28. Liu, Y.; Zhao, X.; Wu, D.; Li, D.; Li, X. Study on the control methods of a water hydraulic variable ballast system for submersible vehicles. *Ocean Eng.* **2015**, *108*, 648–661, doi:10.1016/j.oceaneng.2015.08.045.
29. Liu, F.; Cui, W.; Li, X. China’s first deep manned submersible, JIAOLONG. *Sci. China Earth Sci.* **2010**, *53*, 1407–1410, doi:10.1007/s11430-010-4100-2.
30. Worall, M.; Jamieson, A.J.; Holford, A.; Neilson, R.D.; Player, M.; P.M. Bagley. A variable buoyancy system for deep ocean vehicles. In Proceedings of the OCEANS 2007—Europe, IEEE, Piscataway, NJ, USA, 18–21 June 2007; pp. 1–6, doi:10.1109/OCEANSE.2007.4302317.
31. Steenson, L.V.; Turnock, S.R.; Phillips, A.B.; Harris, C.; Furlong, M.E.; Rogers, E.; Wang, L.; Bodles, K.; Evans, D.W. Model predictive control of a hybrid autonomous underwater vehicle with experimental verification. *Proc. Inst. Mech. Eng. Part M- J. Eng.* **2014**, *228*, 166–179, doi:10.1177/1475090213506185.
32. Fossen, T.I.; Foss, B.A. Sliding control of MIMO nonlinear systems. *Model. Identif. Control.* **1991**, *12*, 129–138, doi:10.4173/mic.1991.3.3.
33. Wang, L. *Model Predictive Control System Design and Implementation Using MATLAB®*; Springer-Verlag: London, UK, 2009; ISBN 978-1-84882-330-3.

34. Dong, M.; Li, J.; Chou, W. Depth control of ROV in nuclear power plant based on fuzzy PID and dynamics compensation. *Microsyst. Technol.* **2019**, doi:10.1007/s00542-019-04605-x.
35. Jin, S.; Kim, J.; Kim, J.; Seo, T. Six-degree-of-freedom hovering control of an underwater robotic platform with four tilting thrusters via selective switching control. *IEEE-ASME Trans. Mechatron.* **2015**, *20*, 2370–2378, doi:10.1109/TMECH.2014.2378286.
36. Fossen, T.I. *Handbook of Marine Craft Hydrodynamics and Motion Control*, 1st ed.; John Wiley & Sons Ltd.: Chichester, UK, 2011; ISBN 978-1-119-99149-6.
37. Liceaga-Castro, E.; van Der Molen, G. A submarine depth control system design. *Int. J. Control.* **1995**, *61*, 279–308, doi:10.1080/00207179508921904.
38. Hobson, B.W.; Bellingham, J.G.; Kieft, B.; McEwen, R.; Godin, M.; Zhang, Y. Tethys-class long range AUVs-extending the endurance of propeller-driven cruising AUVs from days to weeks. In Proceedings of the 2012 IEEE/OES Autonomous Underwater Vehicles (AUV), Southampton, UK, 24–27 September 2012; pp. 1–8, doi:10.1109/AUV.2012.6380735.



© 2020 by the authors. Licensee MDPI, Basel, Switzerland. This article is an open access article distributed under the terms and conditions of the Creative Commons Attribution (CC BY) license (<http://creativecommons.org/licenses/by/4.0/>).